A new ignition hohlraum design for indirect-drive inertial confinement fusion*

Xin Li(李欣), Chang-Shu Wu(吴畅书), Zhen-Sheng Dai(戴振生)†, Wu-Di Zheng(郑无敌), Jian-Fa Gu(谷建法), Pei-Jun Gu(古培俊), Shi-Yang Zou(邹士阳), Jie Liu(刘杰), and Shao-Ping Zhu(朱少平)

Institute of Applied Physics and Computational Mathematics, Beijing 100094, *China*

(Received 16 May 2016; revised manuscript received 2 June 2016; published online 25 July 2016)

In this paper, a six-cylinder-port hohlraum is proposed to provide high symmetry flux on capsule. It is designed to ignite a capsule with 1.2-mm radius in indirect-drive inertial confinement fusion (ICF). Flux symmetry and laser energy are calculated by using three-dimensional view factor method and laser energy balance in hohlraum. Plasma conditions are analyzed based on the two-dimensional radiation-hydrodynamic simulations. There is no Y_{lm} ($l \leqslant 4$) asymmetry in the six-cylinder-port hohlraum when the influences of laser entrance holes (LEHs) and laser spots cancel each other out with suitable target parameters. A radiation drive with 300 eV and good flux symmetry can be achieved by using a laser energy of 2.3 MJ and peak power of 500 TW. According to the simulations, the electron temperature and the electron density on the wall of laser cone are high and low, respectively, which are similar to those of outer cones in the hohlraums on National Ignition Facility (NIF). And the laser intensity is also as low as those of NIF outer cones. So the backscattering due to laser plasma interaction (LPI) is considered to be negligible. The six-cyliner-port hohlraum could be superior to the traditional cylindrical hohlraum and the octahedral hohlraum in both higher symmetry and lower backscattering without supplementary technology at an acceptable laser energy level. It is undoubted that the hohlraum will add to the diversity of ICF approaches.

Keywords: ICF, hohlraums, ignition, six-cylinder port

PACS: 52.57.–z, 52.57.Bc, 52.38.Dx **DOI:** 10.1088/1674-1056/25/8/085202

1. Introduction

The primary route to ignition and high gain in inertial confinement fusion (ICF) involves the use of hohlraums.[1] A hohlraum consists a high Z case with laser entrance holes (LEHs). The laser beams are efficiently converted into x rays at the beam spots on the hohlraum wall. The study and design of a hohlraum target are essentially important in inertial fusion because it seriously influences the capsule symmetry and the hohlraum energetics, which are the most important issues of inertial fusion.[1–3] Typical capsule convergence ratios range from 25 to 45, so that drive asymmetry can be no more than 1%,[1] a demanding specification for hohlraum design. The flux symmetry is strongly dependent on hohlraum geometry and laser beam arrangement. Up to now, various designs with different hohlraum geometries and beam arrangements have been proposed and investigated, such as cylindrical hohlraums[1,3] and spherical hohlraums with 4 LEHs[4,5] or 6 LEHs.[6–8] The cylindrical hohlraums are used most often in inertial fusion studies and are chosen as the ignition hohlraums on the US National Ignition Facility (NIF).[3] In cylindrical hohlraums, the Legendre polynomial modes P_2 and P_4 of the flux on capsule are the main asymmetry modes required to be controlled. The P_2 asymmetry is controlled by using two rings per side in the hohlraum and by adjusting the power ratio between the two rings, the approach that is called beam phasing technology, on NIF.[9] However, the laser beams injected at inner cones encounter complicated laser plasma interaction (LPI) issues,[1] which reflects laser energy out of hohlraum directly and reduces the effect of the beam phasing technology. A crossed-beam energy transfer (CBET) [10] technique is used to maintain the required symmetry. It makes asymmetry control on NIF more complicated. The recent work[11] on NIF showed that the fusion fuel gains exceed unity by using a high-foot implosion method to reduce instability in the implosion., and the hot spot at band-time is still far from a sphere due to the neutron image. The analysis showed that the P_2 symmetry of capsule is as high as -34%. This result shows that the capsule asymmetry is a still serious issue, which must be solved in future.

The spherical hohlraum with 4 LEHs[4,5] has no Y_{2m} spherical harmonic asymmetry, but there exits Y_{3m} asymmetry and it cannot be eliminated by adjusting the target parameters. In the spherical hohlraum[6–8] with 6 LEHs of octahedral symmetry (octahedral hohlraums), the three-dimensional (3D) laser arrangement shows that some laser beams are likely to be blocked by the high-Z plasmas created by other laser spots, which are just above these beams, destroying the symmetry control scheme. And some laser spots are very close to their neighbor LEHs in those hohlraums. Considering the nominal beam pointing errors, these laser beams are likely to

*Project supported by the National Natural Science Foundation of China (Grant Nos. 11435011 and 11575034).

†Corresponding author. E-mail: dai_zhensheng@iapcm.ac.cn

© 2016 Chinese Physical Society and IOP Publishing Ltd

transfer outside hohlraum directly. The high laser intensity of the octahedral hohlraum, due to the small laser spot, can result in high LPI risk, since LPI linear gains is proportional to the laser intensity.[1] And the laser beams are likely to be absorbed by the plasma at LEH due to the very small LEH radius. Besides, when the LEHs are not placed at the specific hohlraum-to-capsule radius ratio of 5.14,[6] there is a residual Y_{4m} asymmetry and it is difficult to eliminate this asymmetry by adjusting target parameters.

In this paper, we investigate a hohlraum with six cylinder ports from theoretical side, addressing the most important issues of the flux symmetry, laser energy, and LPI.

2. Target study

We consider a six-cylinder-port hohlraum with 192 laser beams for a capsule of 1.2-mm radius which is designed for a 300-eV radiation drive. The details of capsule are not discussed here.

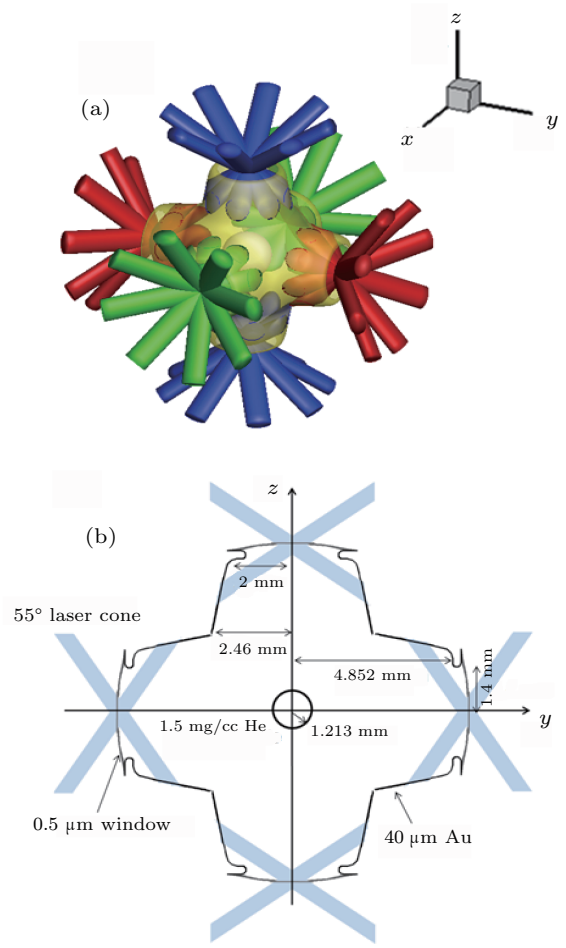


Fig. 1. (color online) (a) Scenography of the hohlraum with six cyliner ports, 48 laser quads and centrally located fusion capsule. (b) Hohlraum specifications.

Shown in Fig. 1 is the scenography of the six-cylinder-port hohlraum and its specifications. The 192 beams are clustered in 48 quads of four beams.[1,3] Eight laser quads entering into each LEH are in one cone at $\theta_L = 55°$ as the opening angle, the angle that is included between the laser quad beam and the LEH normal direction. The laser power is shaped to meet the requirement of capsule with a peak power of 500 TW and total laser energy of 2.3 MJ. Shown in Fig. 2 are the laser profile, the resulting temperature in the hohlraum from simulations and the temperature required by the capsule. Each quad is focused on an elliptical spot, which reduces laser intensity and the long axis of the ellipse is chosen so there is no loss of LEH clearance. The nominal spot is 400 μm × 600 μm at the best focus. The LEH size is designed to prevent laser from being absorbed in the plasma of LEH edges. We choose the LEH radius at $R_{LEH} = 1400$ μm, which is much larger than that in the octahedral hohlraum.[6–8] So our hohlraum has lower laser entering risk than the octahedral hohlraum. The hohlraum material is gold and the hohlraum is filled with helium gas with density 1.5 mg/cc which is confined by a window over the LEH. The gas tamps the motion of the wall and helps to improve laser propagation.[1]

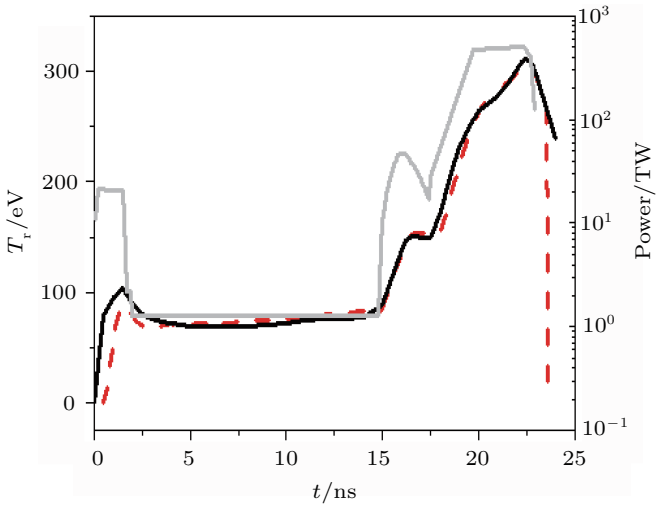


Fig. 2. (color online) Laser power to drive the target (grey, right scale), the resulting temperature in the hohlraum from simulations (black, left scale), and the temperature required by the capsule with 1.2-mm radius (red, left scale).

As described in Ref. [12], there is an optimal configuration of N_L LEHs on an outer sphere with radius R_{outer}, in which the total quantity of the N_L LEHs $a_l^{LEH,total}$, from $l = 1$ to $l = l_0$ ($l_0 = 3$ when $N_L = 6$), are all zero, and $a_{l_0+1}^{LEH,total} \neq 0$.

$$a_l = \sqrt{\sum_{m=-l}^{l} |a_{l,m}|^2}$$

is chosen to describe the l-order flux asymmetry, where $a_{l,m}$ is spherical harmonic decomposition of the flux after removing a "closed total hohlraum wall" flux.[12] Because the smooth factor vanishes quickly for large l, $a_{l_0+1}^{LEH,total}$ dominates the asymmetry modes for $l > l_0$. Reference [12] also points out that a ring of N_s identical spots incident from an LEH is equivalent to an LEH when N_s is greater than some value ($N_s \geqslant 5$ when $N_L = 6$). In our design, the Y_{lm} ($l = 1, 2, 3$) asymmetry contributed by the LEHs and the laser spots are all zero since $N_L = 6$ and $N_s = 8$. From Eq. (17) in Ref. [12], the 4-order contribution $a_4^{spot,total}$ of laser spots, which is proportion

to $P_l(\cos 2\theta_s)$, could be zero at the nodes of $P_4(\cos 2\theta_s)$ at $\theta_s =$ 15.28°, 35.06°, 54.94°, and 74.72°. The angle θ_s is the incident angle included between the laser beam and the LEH normal direction on an outer sphere with radius R_{outer} and $P_l(x)$ is the l-order Legendre polynomial function. $a_4^{spot,total}$ is positive when $\theta_s > 74.72°$. The same equation also shows that the LEH contribution $a_4^{LEH,total} < 0$. The negative sources of LEH and the positive sources of laser spot with $\theta_s > 74.72°$ can cancel each other out to make $a_4^{total} = 0$ ($a_4^{total} = a_4^{spot,total} + a_4^{LEH,total}$). In the six-cylinder-port hohlraum (Fig. 3), the radius $R_{outer,spot}$ of the outer sphere with all laser spots is smaller than the radius $R_{outer,LEH}$ of the sphere with all LEHs. So although the laser incident angle θ_L is 55°, the equivalent laser incident angle θ_s in sphere with $R_{outer,spot}$ is about 80°. It makes the cancelling possible. Instead, in the octahedral hohlraum,[6–8] if $\theta_s > 74.72°$, the laser beams will be very close to the hohlraum wall near LEHs and be prone to being absorbed by the wall blowoff plasma near LEHs.

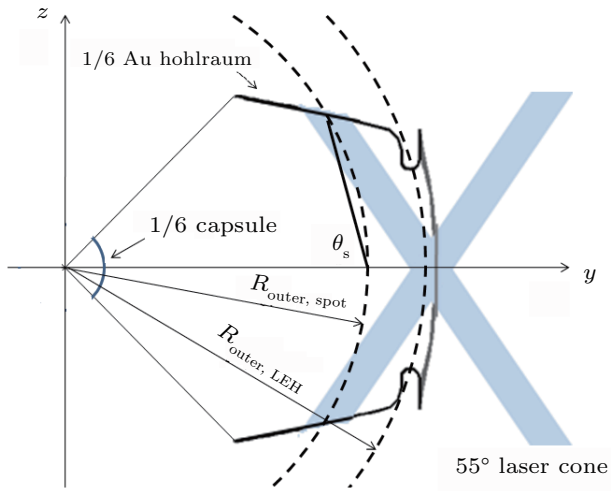


Fig. 3. (color online) Scenography of one single port.

To verify the above theoretical prediction, we further use a 3D view factor code, based on Ref. [13], to calculate the radiation flux on the capsule. The asymmetry of flux on capsule can be decomposed into the spherical harmonics defined in quantum mechanics and b_{lm} is defined as harmonic decomposition. We further define $C_{lm} = b_{lm}/b_{00}$ to describe the quantity of the Y_{lm} asymmetry. Shown in Fig. 4 is the flux distribution on the capsule of 1.2-mm radius. Although the LEHs with $R_{outer,LEH}/R_C = 4$ are not at the node of Y_{4m} smooth factor, we can obtain $C_{4m} \sim 0$. We adjust the length of port, the radius of port, the incident angel of laser quad, and the position of laser ring to achieve the high flux symmetry. Of course, while a large number of target parameters are adjusted to meet the symmetry requirement of capsule, the laser energy should be acceptable during the whole adjusting procedure. According to Ref. [12], the Y_{lm} ($l = 1,2,3$) asymmetries contributed by the LEHs and the laser spots are all absolutely zero in the whole laser duration because the LEHs and the laser spots maintain octahedral symmetry over time, respectively. Y_{4m} is the only remaining asymmetry, which varies with time because the positions of laser spots change over time due to the wall motion. Just like cylindrical hohlraums,[1,3] we can only adjust time-integrated Y_{4m} asymmetry in a six-cylinder port hohlraum mainly by changing the initial positions of the laser spots. In our target design, the laser spots move to about 300 μm away from the LEHs as indicated by analyzing the simulation results (see below) during the whole laser duration. Considering the motion of the laser spots, the 3D view factor calculations show that the Y_{4m} asymmetry varies from 1% to 0 (about 1% at the first two nanoseconds and about zero in the main pulse). And the values of Y_{4m} are much better than the symmetry demands of our ignition capsule (The details of the capsule will be discussed in another paper).

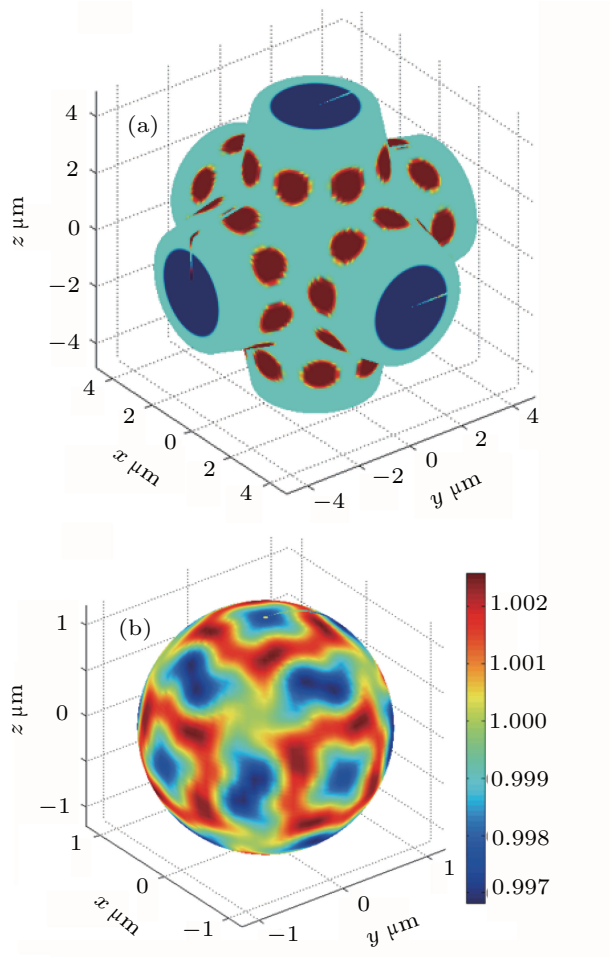


Fig. 4. (color online) (a) Spot pattern on the wall of the six-cylinder-port hohlraum. (b) The relative flux ($F/\bar{F}$) distribution on the capsule with 1.2-mm radius. $\bar{F}$ is the averaged flux.

We use the energy balance[1] to relate the internal hohlraum radiation temperature to the input laser energy by balancing the absorbed laser energy with the x-ray energy radiated into the wall, E_W, absorbed by the capsule, E_C, and the energy that escapes through the LEH, E_{LEH}, i.e.,

$$\eta_{CE}\eta_a E_L = E_W + E_C + E_{LEH}, \quad (1)$$

where η_a is the absorbed laser efficiency and η_{CE} is the x-ray conversion efficiency from laser energy to soft x-rays. $E_W \propto \tau^{0.56} T_r^{3.45} A_W$, $E_C \propto \tau T_r^4 A_C$, and $E_{LEH} \propto \tau T_r^4 A_{LEH}$, where τ is the main pulse duration, T_r the peak radiation temperature, A_W the hohlraum wall area, A_C the capsule area, and A_{LEH} the LEH area. Usually, η_{CE} is around 90% on NIF.[8,14] NIF experimental results[15] of cylindrical hohlraums shows that η_a is about 85%. The 15% loss is almost from the inner cones due to Simulated Raman Scattering (SRS) during peak laser power, and the outer cones have little energy losses. In our target design, each port has one cone and its incident angle, laser intensity and plasma conditions are all similar to those of outer cones of cylindrical hohlraums on NIF. So η_a of hohlraum with 6 cylinder ports should be higher than that of cylindrical hohlraum. In this study, $\eta_a \sim 1$. We apply this energy balance to the ignition target hohlraum with six cylinder ports and find that 2.3-MJ laser energy is required to produce 300-eV peak radiation temperature.

To study the plasma conditions of the cylinder ports by simulations, we consider one cylinder port with 1/6 laser energy on one cone in cylindrical symmetry, because we do not have a 3D hydrodynamics code for the six-cylinder-port hohlraum. The 1/6 capsule is inside the cylinder port. This simulation scheme is reasonable since the six cylinder ports are relatively independent of each other. It is noticeable that the sum of six single cylinder ports is not equivalent to the hohlraum with six cylinder ports, but their differences are too small to influence the plasma conditions and the energy balance very much. We use a 2D non-equilibrium radiation hydrodynamics code LARED-Integration.[16] Capsule needs a shaped radiation temperature to launch sequential shocks.[1] In our design, laser power is tuned to meet the driven temperature requirement of the capsule with 1.2-mm radius. Shown in Fig. 2 are the laser power put into the port and the radiation temperature calculated by simulations. From simulations, the peak power and the total laser energy of the sum of six single ports are 500 TW and 2.4 MJ, which is close to the energy estimated by energy balance.

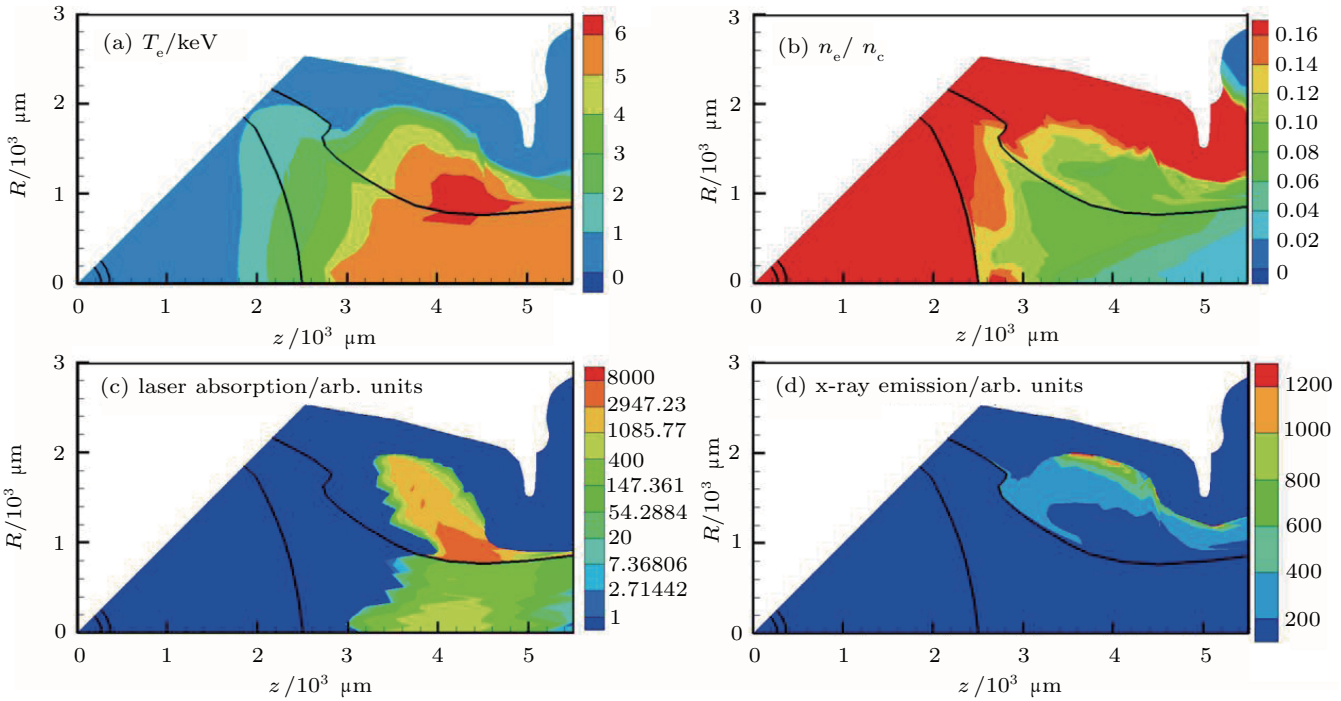


Fig. 5. (color online) Maps of plasma at peak power: (a)$T_e$in keV. (b) n_e/n_c. (c) Laser asorption.(d) x-ray emission.

Maps of the spatial distributions of the electron density, the electron temperature, the x-ray emission, and the laser absorption at peak power are shown in Fig. 5. The laser beams (with laser intensity at $I_L \sim 9.5 \times 10^{14}$ W/cm^2) impact the Au hohlraum wall and create an Au-plasma with high electron temperature ($T_e \sim 6.5$ keV) and low density ($n_e \sim 0.09 n_c$). Here, n_c is the laser critical density. For a laser wavelength λ in microns, $n_c(\text{cm}^{-3}) = 1.1 \times 10^{21}/\lambda(\mu\text{m})^2$. The electron temperature, the electron density, the plasma length (L) and the laser intensity on laser cone are very similar to those on outer cones of cylindrical hohlraums[17] at 300 eV of radiation temperature. The linear gain[18] of simulated Brillouin scattering (SBS) is proportional to $I_L L n_e/T_e$. The analysis[17] shows that SBS rising from Au plasma is the main LPI risk on outer cones of cylindrical hohlraums on NIF. Since experiment results[15] on NIF do not show obvious SBS on outer cones of cylindrical hohlraums, there should be little SBS in the laser beams of the six-cylinder-port hohlraum. That is why we supposed $\eta_a \sim 1$ before.

Without filling the gas, for laser pulse duration as long

as those required for ignition, the Au blowoff driven by laser and radiation has time to fill the hohlraum, and the laser beam will not propagate to the initial impacting point since it is absorbed by the Au plasma filled in the hohlraum. This changes the x-ray emission position and destroys the symmetry control scheme. In our design, He gas at 1.5-mg/cc initial density holds back the Au blowoff and ensures that the path of laser cone is clear (Fig. 5(c)) and the x-ray emission position is very close to the initial laser impacting points (Fig. 5(d)). This is the reason why we can use the view factor code to study the flux asymmetry on capsule.

3. Conclusions

In this work, we propose a new ignition hohlraum with six cylinder ports for the capsule with 1.2-mm radius. We use the 3D view factor calculations, the energy balance analysis, and the 2D hydrodynamic simulations to study the hohlraum. Our theoretical study shows that the six-cylinder-port hohlraum has very high flux symmetry on capsule. Specially, the Y_{4m} asymmetry, which exists in the octahedral hohlraum, can be adjusted to zero by cancelling the influences of laser spots and LEHs each other out, even though the LEHs are not on a sphere with golden radius ratio. About 2.3-MJ laser energy is required to provide the radiation driven of capsule. The simulations show that the plasma conditions in the hohlraum should simulate little SBS and the x-ray emission positions are still very close to the initial ones. Obviously, in addition to the residual Y_{4m} problem, the other problems about laser transferring and LPI, mentioned before in the octahedral hohlraums, are solved or eased in the six-cylinder-port hohlraum. Next, we plan to study more in depth the time-varing Y_{4m} asymmetry, the asymmetry of M-band flux and the laser beam entering problem because there is much room for optimization in the target design. Of course, in future, 3D simulations are necessary to classify the details of asymmetry, plasma, and efficiency in hohlraums. And aboundant experiments are worthy to be done with six-cylinder-port hohlraums on exiting facilities, since we have little experience of laser arrangement, target fabrication, and diagnostics.

Acknowledgment

The authors wish to thank Hao Duan, Hua-Sen Zhang, Yi-Qing Zhao and Ke Lan for beneficial discussion.

References

[1] Lindl J D, Amendt P, Berger R L, Glendinning S G, Glenzer S H, Haan S W, Kauffman R L, Landen O L and Suter L J 2004 *Phys. Plasmas* **2** 3933
[2] Atzeni S and Meyer-ter-Vehn J 2004 *The Physics of Inertial Fusion* (Oxford: Oxford Science Press)
[3] Haan S W, Lindl J D, Callanhan D A, Clark D S, Salmonson J D, Hammel B A, Atherton L J, Cook R C, Edwards M J, Glenzer S, Hamza A V, Hatchett S P, Herrmann M C, Hinkel D E, Ho D D, Huang H, Jones O S, Kline J, Kyrala G, Lanen O L, MacGowan B J, Marinak M M, Meyerhofer D D, Milovich J L, Moreno K A, Moses E I, Munro D H, Nikroo A, Olson R E, Peterson K, Pollaine S M, Ralph J E, Robey H F, Spears B K, Springer P T, Suter L J, Thomas C A, Town R P, Vesey R, Weber S V, Wilkens H L and Wilson D C 2011 *Phys. Plasmas* **18** 051001
[4] Phillion D W and Pollaine S M 1994 *Phys. Plasmas* **1** 2963
[5] Schnittman J D and Craxton R S 1996 *Phys. Plasmas* **3** 3786
[6] Lan K, Liu J, Lai D X, Zheng W D and He X T 2014 *Phys. Plasmas* **21** 010704
[7] Lan K, He X T, Liu J, Zheng W D and Lai D X 2014 *Phys. Plasmas* **21** 052704
[8] Lan K and Zheng W D 2014 *Phys. Plasmas* **21** 090704
[9] Kyrala G A, Kline J L, Dixit S, Glenzer S, Kalantar D, Bradley D, Lzumi N, Meezan N, Landen O, Callahan D, Weber S V, Holder J P, Glenn S, Edwards M J, Koch J, Suter L J, Haan S W, Town R P J, Michel P, Jones O, Langer S, Moody J D, Dewald E L, Ma T, Ralph J, Hamza A, Dzenitis E and Kilkenny J 2011 *Phys. Plasmas* **18** 056307
[10] Michel P, Glenzer S H, Divol L, Bradley D K, Callahan D, Dixit S, Glenn S, Hinkel D, Kirkwood R K, Kline J L, Kruer W L, Kyrala G A, LePage S, Meezan N B, Town R, Widmann K, Williams E A, MacGowan B J, Lindl J and Suter L J 2010 *Phys. Plasmas* **17** 056305
[11] Hurricane O A, Callahan D A, Casey D T, Celliers P M, Cerjan C, Dewald E L, Dittrich T R, Doppnerl T, Hinkel D E, Berzak Hopkins L F, Klines J L, LePage S, Ma T, MacPhee A G, Milovich J L, Pak A, Park H S, Patel P K, Remington B A, Salmonson J D, Springer P T and Tommasini R 2014 *Nature* **506** 343
[12] Duan H, Changshu Wu, Wenbing Pei and Shiyang Zou 2015 *Phys. Plasmas* **22** 092704
[13] Cohen D H, Landen O L and MacFarlane J J 2005 *Phys. Plasmas* **12** 122703
[14] Olson R E, Suter L J, Kline J L, Callahan D A and Rosen M D 2012 *Phys. Plasmas* **19** 053301
[15] Lindl J, Landen O, Edwards J, Moses E and NIC Team 2014 *Phys. Plasmas* **21** 020501
[16] Song P, Zhai C L, Li S G, Yong H, Qi J, Hang X D, Yang R, Cheng J, Zeng Q H, Hu X Y, Wang S, Shi Y, Zheng W D, Gu P J, Zou S Y, Li X, Zhao Y Q, Zhang H S, Zhang A Q, An H B, Li J H, Pei W B and Zhu S P 2015 *High Power Laser and Particle Beams* **27** 032007
[17] Hinkel D E, Haan S W, Langdon A B, Dittrich T R, Still C H and Marnak M M 2003 *Phys. Plasmas* **11** 1128
[18] Laffite S and Loiseau P 2010 *Phys. Plasmas* **17** 102704